

Cauchy Pressure and Valence Electron Concentration Dominated Hardness of Multi-principal Element Carbides Ceramics

Zhigang Ding*, Weian Zhu, Junhao Su, Xuexi Wang, Yicheng Wang, Gaoyuan Zhang

Nano and Heterogeneous Materials Center, School of Materials Science and Engineering, Nanjing University of Science and Technology, Nanjing, Jiangsu 210094, China

***Corresponding to:** Zhigang Ding, Nano and Heterogeneous Materials Center, School of Materials Science and Engineering, Nanjing University of Science and Technology, Nanjing, Jiangsu 210094, China. Email: zhigangding@njust.edu.cn

Abstract: Recent studies indicate that multi-principal element carbides (MPECs) ceramics can simultaneously possess high hardness and high toughness, which have potential applications in industrial fields. Nevertheless, microstructural origins of the excellent hardness and toughness combination remain unclear. In present study, the hardness of 38 derivatives based on (Ti-Zr-Hf-V-Nb-Ta)C MPECs were researched by density functional theory calculations. We found that the non-linear equation combination by Cauchy pressure P_c and valence electron concentration (VEC) show high prediction accuracy ($R^2 = 0.91$) with DFT values. The multivariate regression surface of hardness reveals that high hardness is often associated with high VEC and low Cauchy pressure, which can be used to predict the hardness of MPECs.

Keywords: Multi-principal element carbides; Hardness; Elastic properties; Cauchy pressure; Density functional theory

1. Introduction

Transition metal carbides (TMCs) are among the hardest known compounds, with several binary carbides having high hardness and high melting temperature^[1, 2]. However, the TMCs are prone to oxidation at intermediate temperatures, which cannot fulfill the necessary requirements^[3, 4]. A promising way to explore new TMCs, motivated by the discovery of multi-principal element alloys (MPEAs) is bulk multi-principal element carbides (MPECs)^[2, 5-9]. These MPECs are composed of two to six different

transition metal elements of equimolar proportions and carbon atoms, with rock salt solid solution structures. At the early stage, (Hf-Ta-Zr-Nb)C and (Hf-Ta-Zr-Nb-Ti)C, were successfully synthesized in experiment, the as-prepared metal carbide MPECs exhibit significantly enhanced hardness and elastic modulus and reduced thermal conductivity compared with their constituent metal carbides^[1, 2, 5, 10-14]. Recently, novel multi-principal materials with high strength^[15], deformation behavior^[16], wear resistance^[17], corrosion resistance^[18], irradiation resistance^[19, 20], have been



© The Author(s) 2025. **Open Access** This article is licensed under a Creative Commons Attribution 4.0 International License (<https://creativecommons.org/licenses/by/4.0/>), which permits unrestricted use, sharing, adaptation, distribution and reproduction in any medium or format, for any purpose, even commercially, as long as you give appropriate credit to the original author(s) and the source, provide a link to the Creative Commons license, and indicate if changes were made.

observed. As such, many experimental and theoretical studies have been devoted to correlate the intrinsic physical and chemical characteristic with mechanical properties, which can not only identify the fundamental determinants of mechanical properties but also pave the ways of fast design MPECs.

The hardness enhancement in MPECs has been reported to be associated with the solid solution strengthening in previous works^[5, 21]. However, certain alloys display significant enhancement over the rule of mixtures predicted values, which cannot be fully explained by traditional solid solution strengthening mechanisms^[1]. It has also been suggested that hardness of MPECs decreases as a function of valence electron concentration (VEC)^[13]. Experimental results show a general trend of decreasing hardness in MPECs with increasing VEC, but exists significant deviations amongst multiple systems with same VEC^[1]. For example, TiC, ZrC, and HfC, with same VEC show large deviation in hardness (25-32 GPa, 23-25 GPa, and 16-25GPa, respectively)^[1]. This deviation was proposed to origin from the bond covalency and elasticity properties. TiC exhibits greater bond directionality and higher G/B ratios, due to smaller atomic radius and enhanced orbital overlap of Ti. This suggests that the hardness of MPECs are at least partially dependent on the VEC parameter and elastic characteristics of each of the constituent elements and carbon. Although hardness enhancement in HECs have been reported, an in-depth understanding on how combined elements affect mechanical properties of MPECs are far from completed.

In this article, to clarify the hardness of this interesting new class of MPECs, a family of equiatomic binary, ternary and quaternary MPECs based on the elements Ti, Zr, Hf, V, Nb and Ta were investigated. We found that that Cauchy pressure P_c , shear modulus G , Young's modulus E , and shear strain C_{44} exhibited strong linear correlations with hardness. Furthermore, we found that the non-linear equation combination P_c and VEC show high prediction accuracy with DFT values, which can be used to predict the hardness of MPECs.

2. Computation Approach

We have used the Vienna Ab-initio Simulation Package (VASP) code to perform the DFT calculations^[22].

The projector augmented wave (PAW) method was employed to describe the interactions between the valence electrons and ionic cores^[23]. The standard Perdew-Burke-Ernzerhof (PBE) form of the generalized gradient approximation (GGA) was used as the exchange correction functional^[24]. This functional has been widely used to calculate mechanical properties of transition metal carbides and give good results compare to that of experiments. Pseudopotentials were chosen, following the recommendation by VASP for relatively accurate calculations. To model the random distribution of metal atoms in MPECs, special quasi-random structures (SQSs)^[25] generated by the mcsqs tool in the alloy theoretic automated toolkit (ATAT) code are employed^[26]. In the present study, the $2 \times 2 \times 2$ SQS supercell with 64 atoms was used for all calculations (as shown in **Fig.1(a)** and **(b)**). Atomic positions and lattice parameters were relaxed until an energy convergence of 1 meV/atom was achieved. This was done by multiple calculations for each atomic configuration, where atoms were relaxed at a fixed lattice parameter that was varied for the different calculations by 0.1 Å increments, with the Plane-wave energy cut-off 500 eV and G-centered $5 \times 5 \times 5$ k-meshes. The convergence criterion of energy and force is set to 1.0×10^{-4} eV and 0.5×10^{-3} eV/Å, respectively. Subsequently, the relaxed lattice constant and corresponding energy was fitted by the third-order Birch-Murnaghan equation of state to obtain the equilibrium lattice constant and bulk modulus (B) of alloys. The direction dependent three independent elastic constants for cubic systems C_{11} , C_{12} and C_{44} were calculated by applying a set of strains to the conventional unit cell, and fitting second order polynomial functions to the calculated elastic energy vs strain^[27, 28]. In particular, tensile and compressive ± 1 -3% strains along [001] direction was applied.

We first calculated the equilibrium lattice parameters, bulk modulus, shear modulus, elastic constants and hardness of six single-principal element carbides ceramics. From the elastic constants we see that the Born mechanical stability criteria ($C_{11} > 0$, $C_{44} > 0$, $C_{11}-C_{12} > 0$, $C_{11}+2C_{12} > 0$) is fulfilled for all the considered MPECs, which prove the mechanical stability of these alloys. Then, the equilibrium lattice parameters, bulk modulus, shear modulus, elastic constants and hardness of MPECs were calculated for research the hardness. The calculated hardness values

of TiC, ZrC, HfC, VC, NbC, and TaC are 24.3 GPa, 23.6 GPa, 26.2 GPa, 27.6 GPa, 26.5 GPa, 25.8 GPa, while experiment results are 25-32 GPa, 23-25 GPa, 16-25 GPa, 20-29 GPa, 19-25 GPa, and 16-23 GPa respectively ^[1]. All the calculation results fall within the experimental error range, which demonstrates the efficiency of our DFT calculations.

In the current study, the MPECs are formed by Ti, Zr, Hf, V, Nb and Ta metal elements, which include 57 equal metal atomic MPECs (including 15 binary MPECs, 20 ternary MPECs, 15 quaternary MPECs, 6 quinary and 1 senary MPECs). In our DFT calculation, each system required 28 DFT calculations (e.g., elastic constants, bulk/shear moduli) at ~2 hours per structure (16 CPU cores), totaling 896 core-hours. To reduce computing costs and save time, we performed DFT calculations for selected 38 systems (For details see supplementary information). In the systems, every metal element has similar occurrence probability range from 15% to 20%, which ensure the systems can provide a justification to other compositions. Our DFT calculations predicted a hardness of 24.4 GPa for (TiZrHfNbTa)C, which matches well with the experiment value of 22-32 GPa ^[1]. Similarly, the calculated hardness values of (ZrNbTiV)C and (TiVNbHfTa)C also agree well with the experimental results (24.2 GPa vs. 30 GPa for (ZrNbTiV)C; 26.3 GPa vs. 29 GPa for (TiVNbHfTa)C) ^[14]. Overall, our DFT calculations for MPECs have shown good agreement with literature values, giving us confidence in the accuracy of our results.

The Cauchy pressure (P_c) which reflect the material's plasticity and toughness, can be estimated by the difference of C_{12} and C_{44} as:

$$P_c = C_{12} - C_{44}$$

when it is greater than 0, it indicates that the material is ductile, if it is less than 0, it suggests that the material exhibits brittleness. The more positive and the larger its value, the better the ductility. The polycrystalline shear modulus (G) can be estimated as an average of the upper (G_V) and lower (G_R) bounds according to the Hill averaging method ^[29, 30]:

$$G_V = \frac{(C_{11} - C_{12} + 3C_{44})}{5}$$

$$G_R = \frac{5(C_{11} - C_{12})C_{44}}{4C_{44} + 3(C_{11} - C_{12})}$$

$$G = \frac{G_V + G_R}{2}$$

Pugh's ratio κ and isotropic Poisson's ratio were calculated using $\kappa = G/B$ and $\nu = E/2G - 1$. The Vicker's hardness was calculated according to Tian's model $H_V = 0.92k^{1.137}G^{0.708}$ ^[31].

3. Results and Discussion

To analyze the factors that influence the mechanical properties of MPECs, the deviation between rule of mixtures (ROM) and DFT calculated lattice constants and hardness are discussed. **Fig. 1(c)** shows the lattice constants of all the MPECs calculated by ROM compared with that by DFT. The Pearson (linear) correlation is 0.99, and the square of correlation coefficient R^2 is 0.98. This suggests that lattice constants of MPCs obey ROM, which can be used to fast evaluate lattice constants of MPECs. However, when applying the ROM to hardness, we find large deviation between the DFT and ROM results (see **Fig. 1(d)**). This result indicates that the structural optimization performed on the model during DFT calculations introduces certain lattice distortions in the crystal, which cannot be captured in ROM calculations. This deviation was proposed to origins from the fact that the hardness of MPECs not only from the basic properties of elements by the ROM but also from the mutual interactions among all the elements (such as segregations, structural disorder, and short-range order) ^[32]. Typically, the sluggish diffusion effect on the shear deformation process, which clearly indicates that local atom movement have more effects on shear deformation process and further affects the plastic deformation of MPECs. Therefore, although ROM can predict the lattice constants of MPECs very well, it is not suitable to predict the hardness of MPECs.

To further explore the intricate relationship between material properties and hardness, we conducted a detailed analysis by calculating both the Pearson correlation coefficient (PCC) and the Maximal information coefficient (MIC) of eight key element properties in relation to hardness (see **Fig.2**). This approach allowed us to uncover the connections that might not be apparent through traditional statistical methods alone. The PCC measures a linear relationship between two variables. We observed that P_c (-0.859), G (0.83), E (0.778), and C_{44} (0.753) exhibited strong

linear correlations with hardness. These results suggest that materials with higher values in these properties tend to exhibit greater hardness, which is consistent with theoretical predictions and previous empirical findings. On the other hand, the MIC was employed to identify any potential non-linear relationships that might exist between the element properties and

hardness. We also observed that P_c (0.569), G (0.645), E (0.531), and C_{44} (0.687) exhibited strong correlations with hardness. Considering the MIC did not reveal any significant non-linear correlations beyond those already identified by the PCC, it provided additional confidence in the robustness of our linear correlation findings.

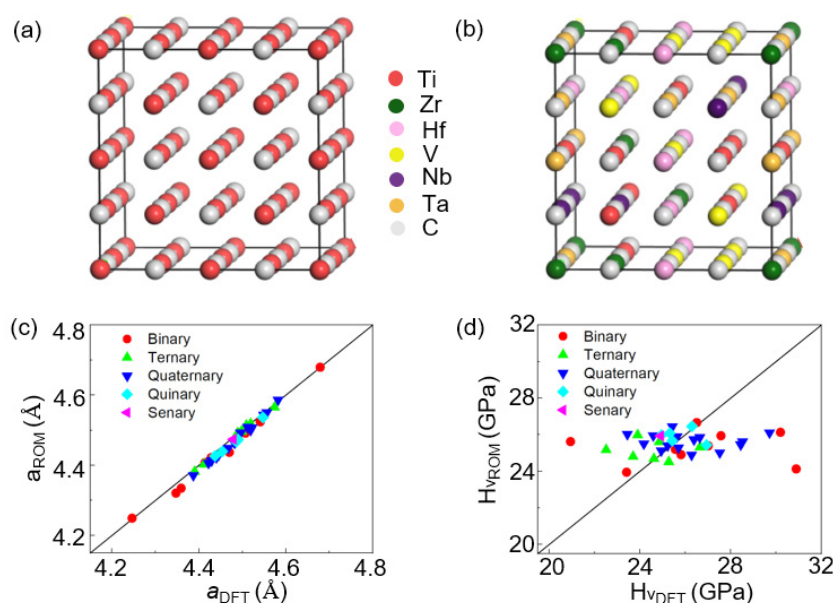


Figure 1 The supercells with 64 atoms was used for all calculations of (a) TMCs and (b) MPECs. Figure (c)-(d) show the deviation between the rule of mixtures (the solid points) predicted values with that of DFT (the solid line) calculations. The large deviation in hardness implicates that rule of mixtures is not suitable to predict the hardness of MPECs.

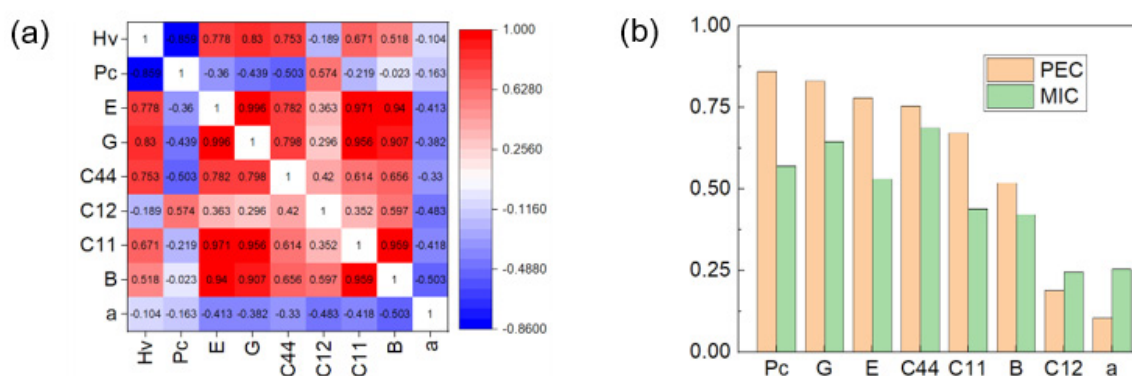


Figure 2 The (a) Pearson correlation coefficient (PCC) and (b) Maximal information coefficient (MIC) of eight key element properties in relation to hardness.

Having identified four key properties strongly correlated with hardness, our next step is to evaluate the performance of these properties in predicting the hardness values of unknown alloys. **Figure 3** illustrates the hardness values calculated using linear relationships derived from these four properties. The red line in this figure represents the predicted hardness values

based on the linear model. To gauge the accuracy of our predictions, the determination coefficient (R^2) was selected to assess the accuracy of the prediction. The metric was chosen for their ability to provide a clear picture of how closely the predicted hardness values align with those obtained through density functional theory (DFT) calculations. As show in **Fig. 3**, the

R^2 is 0.74, 0.69, 0.61, and 0.57 for P_c , G , B , and C_{44} , respectively. This indicates that the Cauchy pressure model exhibits the strongest correlation with the DFT

derived hardness values. However, it is important to note that while the Cauchy pressure performs well, there may still be room for improvement.

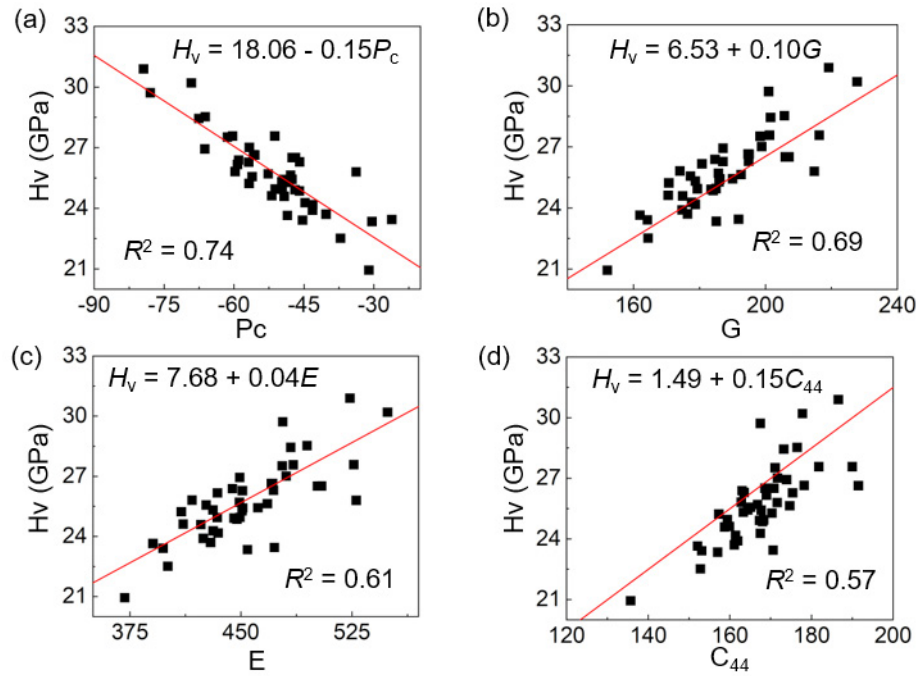


Figure 3 The hardness of MPECs with respect to P_c , G , E , and C_{44} , respectively. The fitting curves are shown as red solid lines, while the fitting functions are also displayed in each graph.

Considering that the hardness of carbides is associated with valence electron concentration (VEC) proposed by Balasubramanian^[13], combination P_c and VEC may further improve the prediction accuracy. **Figure 4** illustrates this concept by presenting a multivariate regression surface predicted using both P_c and VEC as independent variables. The R^2 values obtained from this combined model is 0.91, which show significantly accuracy compared to those derived solely from P_c . To estimate the overfitting introduced by small dataset, we performed 5-fold cross-validation to evaluate the fluctuation of R^2 . By partitioning the dataset into five subsets, we yield the following R^2 scores: 0.69, 0.95, 0.87, 0.80, and 0.93 (mean = 0.85 ± 0.1). While this reveals some degree of overfitting compared to the training score. However, the combined model improvement over the Cauchy stress only baseline ($R^2 = 0.79$), confirming that VEC incorporation meaningfully enhances predictive capability. Furthermore, our analysis reveals that high hardness is often associated with a high VEC coupled with a low P_c . This is different with Balasubramanian's studies^[13],

which show decrease in hardness from 25 GPa to 2 GPa as VEC increased from 8 to 11. Our study focuses specifically on the VEC range of 8-9, which differs from Balasubramanian's broader investigation. We note that within the VEC range of 8-9, both increasing and decreasing hardness trends were observed with increasing VEC in Balasubramanian's studies. Furthermore, Balasubramanian's research examined only binary carbides, nitrides, and carbonitrides, which do not exhibit the pronounced high-entropy effects characteristic of our materials. In our system, the Cauchy pressure demonstrates a more dominant influence on hardness compared to VEC, which shows less significant effects. Therefore, our finding provides valuable insights into the design of new carbide materials with tailored mechanical properties. For instance, by carefully selecting compositions that optimize both P_c and VEC, it may be possible to develop carbides with enhanced hardness and modulus, thereby extending their utility in demanding industrial applications.

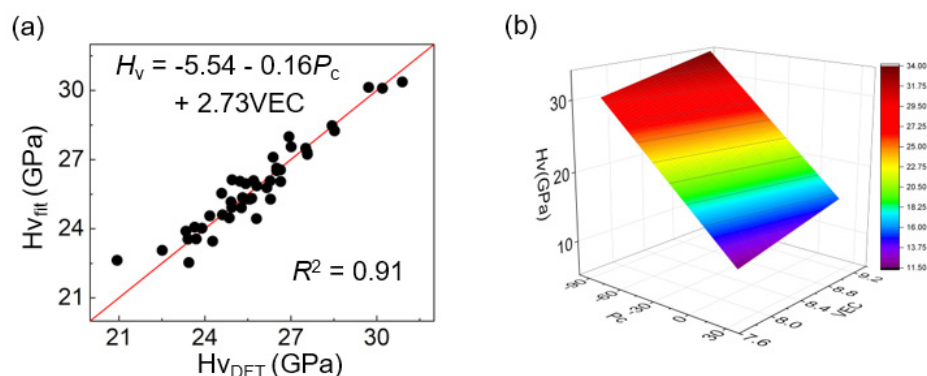


Figure 4 (a) The deviation between the non-linear equation combination P_c and VEC (the solid points) predicted values with that of DFT (the solid line) calculations. while the fitting functions are also displayed in graph. (b) The multivariate regression surface using P_c and VEC as independent variables to predict hardness.

4. Conclusions

We have carried out density functional theory calculations to systematically study the hardness of multi-principal element carbides (MPECs). We found that that non-linear equation combination P_c and VEC show high prediction accuracy ($R^2 = 0.91$) with DFT values, which can be used to predict the hardness of MPECs. We proposed that MPECs with high VEC and low Cauchy pressure associated with high hardness, which provides valuable insights into the design of new MPECs with high hardness.

Acknowledgements

We acknowledge support from the Natural Science Foundation of China (52130110), and the Natural Science Foundation of Jiangsu Province (BK20211198).

References

- [1] Sarker P, Harrington T, Toher C, Oses C, Samiee M, Maria JP, Brenner DW, Vecchio KS, Curtarolo S. High-entropy high-hardness metal carbides discovered by entropy descriptors. *Nature Commun.* 2018;9(1):4980.
- [2] Harrington TJ, Gild J, Sarker P, Toher C, Rost CM, Diplo OF, McElfresh C, Kaufmann K, Marin E, Borowski L, Hopkins PE, Luo J, Curtarolo S, Brenner DW, Vecchio KS. Phase stability and mechanical properties of novel high entropy transition metal carbides. *Acta Mater.* 2019;166:271-280.
- [3] De Leon N, Yu XX, Yu H, Weinberger CR, Thompson GB. Bonding effects on the slip differences in the B1 monocarbides. *Phys. Rev. Letter.* 2015;114(16):165502.
- [4] Li H, Zhang L, Zeng Q, Guan K, Li K, Ren H, Liu S, Cheng L. Structural, elastic and electronic properties of transition metal carbides TMC (TM=Ti, Zr, Hf and Ta) from first-principles calculations. *Solid State Commun.* 2011;151(8):602-606.
- [5] Han X, Girman V, Sedlak R, Dusza J, Castle EG, Wang Y, Reece M, Zhang C. Improved creep resistance of high entropy transition metal carbides. *J Eur. Ceram. Soc.* 2020;40(7):2709-2715.
- [6] Walbrühl M, Linder D, Ågren J, Borgenstam A. A new hardness model for materials design in cemented carbides. *Int J Refract. Met. H.* 2018;75:94-100.
- [7] Yu H, Bahadori M, Thompson GB, Weinberger CR. Understanding dislocation slip in stoichiometric rocksalt transition metal carbides and nitrides. *J Mater. Sci.* 2017;52(11):6235-6248.
- [8] Wang W, Cheng C, Qiao J, Han L, Li Y, Miao Y. Fabrication and mechanical properties of multi-principal cation (Mg,Ti,Cr,Zr,Al,Si) mullite ceramic. *Ceram. Int.* 2024;50(14):25738-25748.
- [9] Wang W, Lian W, Han L, Qiao J, Liaw PK. High-strength and low-thermal-conductivity porous multi-principal cation mullite ceramic. *Ceram. Int.* 2025;51(5):5821-5831.
- [10] Yu XX, Weinberger CR, Thompson GB. Ab initio investigations of the phase stability in group IVB and VB transition metal carbides. *Comput. Mater. Sci.* 2016;112:318-326.

- [11] Maouche D, Louail L, Ruterana P, Maamache M. Formation and stability of di-transition-metal carbides $\text{Ti}_x\text{Zr}_{1-x}\text{C}$, $\text{Ti}_x\text{Hf}_{1-x}\text{C}$ and $\text{Hf}_x\text{Zr}_{1-x}\text{C}$. *Comput. Mater. Sci.* 2008;44(2):347-350.
- [12] Sarker S, Rahman MA, Khatun R. Study of structural, elastic, electronics, optical and thermodynamic properties of Hf_2PbC under pressure by ab-initio method. *Comput. Condens. Matter.* 2021;26:e00512.
- [13] Balasubramanian K, Khare SV, Gall D. Valence electron concentration as an indicator for mechanical properties in rocksalt structure nitrides, carbides and carbonitrides. *Acta Mater.* 2018;152:175-185.
- [14] Ye B, Wen T, Huang K, Wang CZ, Chu Y. First-principles study, fabrication, and characterization of $(\text{Hf}_{0.2}\text{Zr}_{0.2}\text{Ta}_{0.2}\text{Nb}_{0.2}\text{Ti}_{0.2})\text{C}$ high entropy ceramic. *J Am. Ceram. Soc.* 2019;102(7):4344-4352.
- [15] Li Q, Huang Z, Xie M, Ye W, Zhou Q, Qiu L, Qian D, Pinto HC, Song Z, Wang H. A VCoNiN multi-principal nitride film with excellent wear performance. *Surf. Coat. Technol.* 2023;475(25):130130.
- [16] Li S, Zhou Q, Shi Y, Ye W, Lin Y, Wang H. The deformation mechanism of graphene nanosheets embedded in high-entropy alloy upon sliding. *Carbon.* 2024;229:119532.
- [17] Zhou Q, Xia Q, Li Q, Luo D, Huang Z, Wang C, Chen Z, Wang H. Microstructure, mechanical and tribological properties of NbMoWTaAg refractory high entropy films with nano-layered self-organization. *Tribol. Int.* 2024;198:109888.
- [18] Jiao Z, Dong Y, Li Q, Zhou Q, Han S, Yin C, Huang Z, Wang X, Wang H, Liu W. Enhancing tribocorrosion resistance of VCoNi alloys in artificial seawater via nitrogen alloying. *Corros. Sci.* 2025;243:112600.
- [19] Shi Y, Xia Q, Xie M, Zhou Q, Hua D, Chai L, Shi T, Eder SJ, Wang H, Wang P, Liu W. Insights into irradiation-affected structural evolution and mechanical behavior of amorphous carbon. *Acta Mater.* 2024;281:120424.
- [20] Shi Y, Wang W, Zhou Q, Xia Q, Hua D, Huang Z, Chai L, Wang H, Wang P. A Molecular Dynamics Study on the Defect Formation and Mechanical Behavior of Molybdenum Disulfide under Irradiation. *ACS Appl. Mater. Interfaces.* 2024;16(22):29453-29465.
- [21] Zhang Y, Jiang ZB, Sun SK, Guo WM, Chen QS, Qiu JX, Plucknett K, Lin HT. Microstructure and mechanical properties of high-entropy borides derived from boro/carbothermal reduction. *J Eur. Ceram. Soc.* 2019;39(13):3920-3924.
- [22] Kresse G, Furthmüller J. Efficient iterative schemes for ab initio total-energy calculations using a plane-wave basis set. *Phys. Rev. B.* 1996;54(16):11169-11186.
- [23] Blöchl PE. Projector augmented-wave method. *Phys. Rev. B.* 1994;50(24):17953-17979.
- [24] Perdew JP, Burke K, Ernzerhof M. Generalized Gradient Approximation Made Simple. *Phys. Rev. Letter.* 1996;77(18):3865-3868.
- [25] Zunger A, Wei SH, Ferreira LG, Bernard JE. Special quasirandom structures. *Phys. Rev. Letter.* 1990;65(3):353-356.
- [26] Van De Walle A, Tiwary P, De Jong M, Olmsted DL, Asta A, Dick A, Shin D, Wang Y, Chen LQ, Liu ZK. Efficient stochastic generation of special quasirandom structures. *Calphad.* 2013;42:13-18.
- [27] Birch F. Finite Elastic Strain of Cubic Crystals. *Phys. Rev.* 1947;71(11):809-824.
- [28] Murnaghan FD. Finite Deformations of an Elastic Solid. *Am. J Math.* 1937;59(2):235-260.
- [29] Hill R. The Elastic Behaviour of a Crystalline Aggregate. *Proc. Phys. Soc. Sect. A.* 1952;65(5):349-354.
- [30] Zaddach AJ, Niu C, Koch CC, Irving DL. Mechanical Properties and Stacking Fault Energies of NiFeCrCoMn High-Entropy Alloy. *JOM.* 2013;65(12):1780-1789.
- [31] Tian Y, Xu B, Zhao Z. Microscopic theory of hardness and design of novel superhard crystals. *Int J Refract. Met. H.* 2012;33:93-106.
- [32] Ding Z, Zhou J, Yang P, Sun H, Ren JC, Zhao Y, Liu W. Accelerated exploration of high-performance multi-principal element alloys: data-driven high-throughput calculations and active learning method. *Mater. Res. Letter.* 2023;11(8):670-677.